Article

Theoretical Analysis of Factors Controlling the Nonalternating CO/CH Copolymerization

Alicja Haras, Artur Michalak, Bernhard Rieger, and Tom Ziegler

J. Am. Chem. Soc., **2005**, 127 (24), 8765-8774• DOI: 10.1021/ja050861d • Publication Date (Web): 26 May 2005

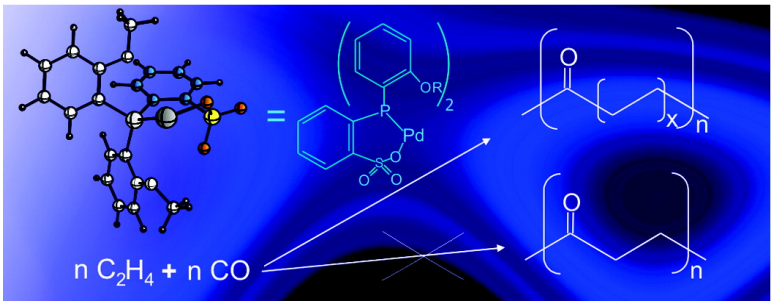

More About This Article

Additional resources and features associated with this article are available within the HTML version:

- Supporting Information
- Links to the 7 articles that cite this article, as of the time of this article download
- Access to high resolution figures
- Links to articles and content related to this article
- Copyright permission to reproduce figures and/or text from this article

View the Full Text HTML

J|A|C|S
ARTICLES
Published on Web 05/26/2005

Theoretical Analysis of Factors Controlling the Nonalternating CO/C_2H_4 Copolymerization

Alicja Haras,[†] Artur Michalak,[†,‡] Bernhard Rieger,[§] and Tom Ziegler*,[†]

Contribution from the Department of Chemistry, University of Calgary, University Drive 2500, Calgary, Alberta, Canada T2N 1N4, Department of Theoretical Chemistry, Jagiellonian University, R. Ingardena 3, 30-060 Cracow, Poland, and Department of Inorganic Chemistry II, Material Science and Catalysis, University of Ulm, 89081 Ulm, Germany

Received February 9, 2005; E-mail: ziegler@ucalgary.ca

Abstract: A [P−O]Pd catalyst based on *o*-alkoxy derivatives of diphenylphosphinobenzene sulfonic acid (I) has recently been shown by Drent et al. (*Chem. Commun.* **2002**, 9, 964) to perform nonalternating CO/C_2H_4 copolymerization with subsequent incorporation of ethylene units into the polyketone chain. The origin of the nonalternation is investigated in a theoretical study of I, where calculated activation barriers and reaction heats of all involved elementary steps are used to generate a complete kinetic model. The kinetic model is able to account for the observed productivity and degree of nonalternation as a function of temperature. Consistent with the energy changes obtained for the real catalyst model, the selectivity toward a nonalternating distribution of both comonomers appears to be mainly a result of a strong destabilization of the Pd−acyl complex.

Introduction

The carbon monoxide and ethylene copolymerization, catalyzed by palladium complexes with chelating phosphine ligands, belongs to one of the most studied reactions in the area of ethylene copolymerization with polar monomers.[1−11] The fact that the resulting polymer offers a unique set of properties for a wide range of applications, while being made from cheap and easily available monomers, makes the process of potential interest for industry.[1,10,12] From an academic point of view, the reaction is remarkable in that a nonuniform distribution of CO and C_2H_4 ($CO:C_2H_4 < 1$) within the growing polymer chain can only be accomplished through radical-initiated polymerization.[1] Excluding one example, which inspired these studies, all catalytic CO/C_2H_4 copolymerization processes are known to provide polyketones with strictly alternating CO/ethylene units even though many of the catalysts are successfully used to oligomerize ethylene.[10,12]

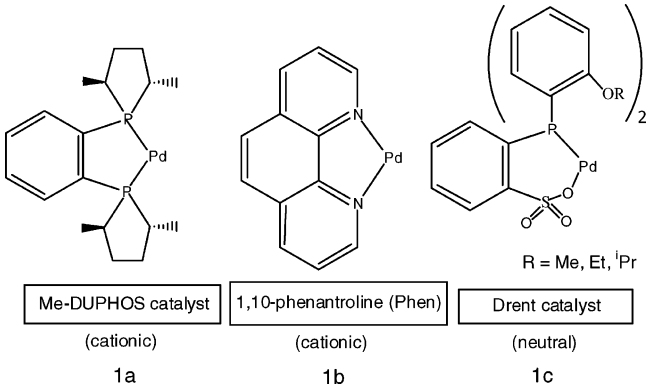

Figure 1. A schematic representation of the cationic systems used as catalysts for the carbon monoxide/ethylene alternating copolymerization (models 1 and 2) together with the catalyst developed by Drent et al.[13] for the nonalternating copolymerization of the comonomers.

Starting from the early papers by Sen,[2,3] there have been many experimental and theoretical studies devoted to rationalize the strictly alternating nature of CO/C_2H_4 coupling based on cationic Pd(II) catalysts with symmetric chelating P−P and N−N ligands (see a and b of Figure 1).

Among them, one should mention the kinetic model proposed by Brookhart et al.[14,15] and the theoretical studies of Margl and Morokuma,[16−18] which have provided valuable information on mechanistic aspects of this process. According to these

† University of Calgary.
‡ Jagiellonian University.
§ University of Ulm.

(1) Sen, A. *Catalytic Synthesis of Alkene−Carbon Monoxide Copolymers and Cooligomers*; Kluwer Academic Publishers: Dordrecht, The Netherlands, 2003.
(2) Sen, A. *Acc. Chem. Res.* **1993**, *26*, 303−310.
(3) Jiang, Z.; Adams, S. E.; Sen, A. *Macromolecules* **1994**, *27*, 2694−2700.
(4) Belov, G. P. *Kinet. Katal.* **2001**, *42*, 301−309.
(5) Belov, G. P. *Russ. Chem. Bull., Int. Ed.* **2002**, *51*, 1605−1615.
(6) Ittel, S. D.; Johnson, L. K.; Brookhart, M. *Chem. Rev.* **2000**, *100*, 1169−1204.
(7) Bianchini, C.; Lee, H. M.; Meli, A.; Oberhauser, W.; Vizza, F.; Brüggeller, P.; Haid, R.; Langes, Ch. *Chem. Commun.* **2000**, *9*, 777−778.
(8) Dossett, S. J.; Gillon, A.; Orpen, A. G.; Fleming, J. S.; Pringle, P. G.; Wass, D. F.; Jones, M. D. *Chem. Commun.* **2001**, *8*, 699−700.
(9) Abu-Surrah, A. S.; Rieger, B. *Top. Catal.* **1999**, *7*, 165−177.
(10) Drent, E.; Budzelaar, P. H. M. *Chem. Rev.* **1996**, *96*, 663−682.
(11) Liu, J.; Heaton, B. T.; Iggo, J. A.; Whyman, R. *Chem. Commun.* **2004**, *11*, 1326−1327.
(12) Liu, W.; Malinoski, J. M.; Brookhart, M. *Organometallics* **2002**, *21*, 2836−2838.
(13) Drent, E.; van Dijk, R.; Ginkel, R.; van Oort, B.; Pugh, R. I. *Chem. Commun.* **2002**, *9*, 964−965.
(14) Rix, F. C.; Brookhart, M.; White, P. S. *J. Am. Chem. Soc.* **1996**, *118*, 4746−4764.
(15) Shultz, C. S.; Ledford, J.; DeSimone, J. M.; Brookhart, M. *J. Am. Chem. Soc.* **2000**, *122*, 6351−6356.
(16) Margl, P.; Ziegler, T. *J. Am. Chem. Soc.* **1996**, *118*, 7337−7344.
(17) Margl, P.; Ziegler, T. *Organometallics* **1996**, *15*, 5519−5523.

studies,[14−18] the double insertion of CO is not observed for thermodynamic reasons. As for the double ethylene insertion, the process is thermodynamically possible, but it does not occur because of the difference in the binding affinity of CO and ethylene to the metal center of the catalyst (kinetic control). In addition, the catalytic metal center is not very tolerant to functionalities present in the growing polymer. Thus, coordination of oxygen from the growing polymer chain takes place, resulting in a higher activation barrier for the ethylene incorporation into the metal−alkyl bond.[16,18] This phenomenon occurs even in the presence of late transition metals, which are known to be much less oxophilic than early transition metals.[6,20]

Drent et al. have reported recently the very first example of nonalternating metal-catalyzed CO/C_2H_4 coupling[13] using a Pd(II) complex with a P−O chelate (see c of Figure 1). The discovery by Drent et al. prompted us to conduct a full theoretical investigation into the new catalytic system in order to understand the experimental results. The random incorporation of CO may potentially have industrial utility because it could lead to novel functionalized polymeric materials with a decreased percentage of CO in the polymer chain.[1] This material might be more stable than polyketone with strictly alternating CO/ethylene incorporation, especially when exposed to high temperatures for extended periods.[21,22] From a fundamental point of view, it is of interest to understand the extent to which one can manipulate the polyketone microstructure.

This account provides a kinetic model for the CO/ethylene copolymerization as well as a general analysis of the electronic and steric factors allowing for the nonalternating CO/C_2H_4 copolymerization to occur in the complex recently designed by Drent[13] (see Figure 1c).

Catalytic Model and Computational Method

The neutral catalyst 1c reported by Drent et al.[13] is based on *o*-alkoxy derivatives of diphenylphosphinobenzene sulfonic acid. A generic model of the catalyst consisting of phosphinobenzene sulfonic acid with two hydrogen atoms at P replacing the *o*-alkoxy diphenyl substituents is shown in Figure 2 as 2a.

Characteristic features of 1c and 2a are the presence in the palladium coordination sphere of heterochelating ligands containing phosphorus (soft donor) and oxygen (hard donor) centers[23] adopting an envelope conformation. The combination of P and O atoms in the palladium coordination sphere gives rise to two possible coordination modes cis or trans to the O donor for the monomers, with different M−L distances.

In addition to the simple catalyst model 2a, in which hydrogen atoms have replaced aryls, we have studied the catalyst 2b with full-size ligands. A view of 2b is given in Figure 2. It is important to note that the bulky groups in 2b of Figure 2 reside only at one arm of the chelate ligand. To simplify the notation, we will hereafter also refer to the H-substituted (2a) and full-size ligand (2b) models as HSM and FSLM, respectively.

The geometries and the electronic structure of the reactants, products, and transition states along the considered reaction paths were determined with the Amsterdam Density Functional suite of programs developed by Baerends et al.[24] To allow for a future comparison with the results of Margl on the cationic Pd catalyst 1, the methodology adopted here is the same as the one employed in refs 15 and 16. In line with Margl, all stationary points were optimized without any geometry constraints using the procedure developed by Versluis and Ziegler.[25,26] Use was made of the local density approximation augmented with the gradient corrections due to Becke (exchange)[27] and Perdew (correlation)[28,29] for both energies and structures. A triple-ζ STO basis set with polarization function was employed for Pd, while all other atoms were described by double-ζ plus polarization STO bases. The first-order scalar relativistic corrections were added to the total energy of the system. Finally, zero-point energy correction (ZPE) was not included to reduce computer time. The error is expected to be acceptable based on related theoretical studies.[30] The approximate reaction paths were evaluated by a linear transit method with the chosen reaction coordinate being the distance between the α-carbon of the growing polymer chain and a carbon atom of the coordinated monomer.

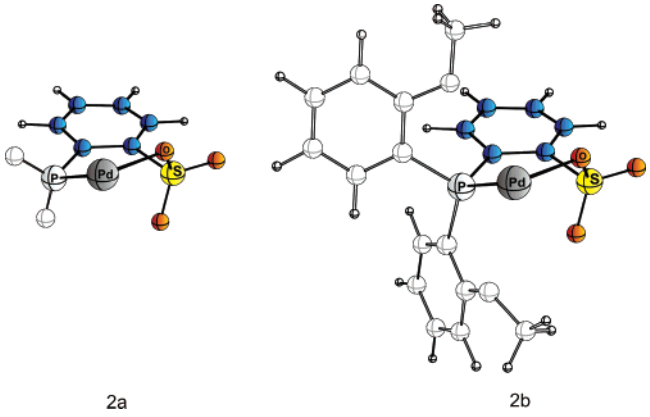

2a 2b

Figure 2. Theoretical model of the catalyst for nonalternating carbon monoxide/ethylene copolymerization developed by Drent et al.,[13] with (a) hydrogens replacing the bulky ligands at the P atom and (b) bis-*o*-methoxy-substituted aryls at the P donor atom. Appropriate atoms are differentiated by the color and size of the spheres: palladium (large, dark gray); phosphorus (medium size, light gray); sulfur (medium size, yellow); oxygen (medium size, red); carbon (medium size, blue), and hydrogen (small size, white).

Kinetic Model

Typically, the alternating CO/C_2H_4 copolymerization is a two-step process involving CO insertion into the alkyl−Pd bond (C → D of Scheme 1) and C_2H_4 insertion into the acyl−Pd bond (E → A of Scheme 1). Kinetic investigations into the mechanism by Brookhart[14,15] analyzed the origin for the perfect alternating copolymerization by considering the competition between the rates of the CO and C_2H_4 incorporations into the Pd−alkyl bond, where the latter insertion would lead to the nonalternating copolymerization. It was assumed in this model that both insertion processes are irreversible. To account for the possibility of the nonalternating copolymerization, we shall extend the original analyses of Brookhart by considering, as well, the reversible decarbonylation (D → C of Scheme 1) of the acyl product formed from insertion of CO into the metal−alkyl bond. We shall still assume that the insertion of ethylene into the metal−alkyl bond is irreversible.

(18) Svensson, M.; Matsubara, T.; Morokuma, K. *Organometallics* **1996**, *15*, 5568−5576.
(19) Sen, A. *Pure Appl. Chem.* **2001**, *73*, 251−254.
(20) Budzelaar, P. H. M. *Organometallics* **2004**, *23*, 855−860.
(21) Severini, F.; Gallo, R.; Brambilla, L.; Castiglioni, C.; Ipsale, S. *Polym. Degrad. Stab.* **2000**, *69*, 133−142.
(22) DeVito, S.; Bronco, S. *Polym. Degrad. Stab.* **1999**, *63*, 399−406.
(23) Lindner, E.; Schmid, M.; Wegner, P.; Nachtigal, Ch.; Steimann, M.; Fawzi, R. *Inorg. Chim. Acta* **1999**, *296*, 103−113.
(24) (a) Baerends, E. J.; Ellis, D. E.; Ros, P. *Chem. Phys.* **1973**, *2*, 41. (b) Baerends, E. J.; Ros, P. *Chem. Phys.* **1973**, *2*, 52. (c) te Velde, G.; Baerends, E. J. *J. Comput. Phys.* **1992**, *99*, 84−98. (d) Fonseca, C. G.; Visser, O.; Snijders, J. G.; te Velde, G.; Baerends, E. J. In *Methods and Techniques in Computational Chemistry, METECC-95*; Clementi, E., Corongiu, G., Eds.; STEF: Cagliari, Italy, 1995; p 305.
(25) Versluis, L.; Ziegler, T. *J. Chem. Phys.* **1988**, *88*, 322−328.
(26) Fan, L.; Ziegler, T. *J. Am. Chem. Soc.* **1992**, *114*, 10890−10897.
(27) Becke, A. D. *Phys. Rev. A* **1988**, *38*, 3098−3100.
(28) Perdew, J. P. *Phys. Rev. B* **1986**, *34*, 7406−7406.
(29) Perdew, J. P. *Phys. Rev. B* **1986**, *33*, 8822−8824.
(30) Schenck, H.; Strömberg, S.; Zetterberg, K.; Ludwig, M.; Kermark, B.; Svensson, M. *Organometallics* **2001**, *20*, 2813−2819.

Scheme 1. Chain Propagation Mechanism for the CO/C_2H_4 Copolymerization Reaction

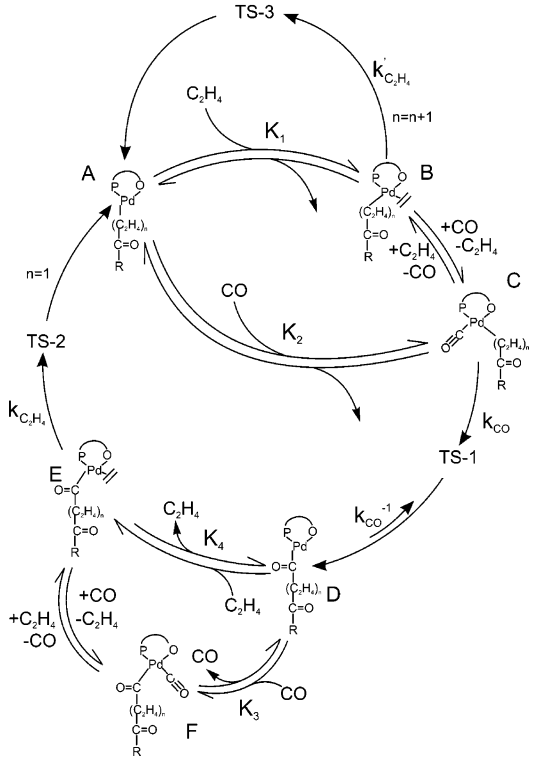

Thus, the overall mechanism closely resembles the one proposed by Brookhart and co-workers[14,15] (see Scheme 1). It assumes equilibrium between associative exchange of C_2H_4 and CO monomers (step 1 from B to C) and two alternative propagation steps:

C_2H_4 migratory insertion into the metal−alkyl bond (step 2 from B to A).

CO migratory insertion into the metal−alkyl bond (step 3 from C to D).

However, due to the fact that the proposed mechanism considers the CO insertion to be reversible, there are additional steps:

Step 4 representing decarbonylation of CO (from D to C).

Step 5 representing equilibrium between the free ethylene and ethylene coordinated to the metal−acyl complex (from D to E).

Step 6 representing equilibrium between free CO molecule and CO coordinated to the metal−acyl (D) complex as F.

Step 7 representing insertion of ethylene into the metal−acyl bond (from E to A).

So, in this mechanism, species related to A are proposed to be either a Pd−acyl system (when $n = 0$) or a Pd−alkyl complex (when $n \geq 1$). The double insertion of carbon monoxide is ignored for thermodynamic reasons. According to Margl,[16] the insertion of a CO−CO unit yields only −88 kJ/mol, whereas insertion of one C_2H_4−CO or C_2H_4−C_2H_4 segment yields −219 or −200 kJ/mol, respectively. Also, double CO insertion has a high barrier (109 kJ/mol).

To describe the chemical transformation, one can apply the steady-state approximation to the concentrations of B, C, D, E, and F in the above mechanism of Scheme 1 and obtain an approximate equation for the ratio (f_{na}) of the overall rates for the nonalternating, $r_{na} = k'_{C_2H_4}$[B], and alternating, $r_a = k_{CO}$[C] − k_{CO}^{-1}[D], paths as

$$f_{na} = \frac{r_{na}}{r_a} = \left(\frac{k'_{C_2H_4}}{k_{CO}}\frac{[C_2H_4]}{[CO]}\frac{K_1}{K_2}\right)\left(1 - \frac{{k_{CO}}^{-1}}{K_4 k_{C_2H_4}[C_2H_4] + {k_{CO}}^{-1}}\right)^{-1} \quad (1)$$

It contains the original expression by Brookhart:

$$\frac{r_{na}}{r'_a} = \frac{k'_{C_2H_4}}{k_{CO}}\frac{[C_2H_4]}{[CO]}\frac{K_1}{K_2} = F_B \quad (2)$$

that was developed based on the assumption that the degree of alternation can be explained in terms of the competition between CO and ethylene insertion into the Pd−alkyl bond without considering decarbonylation, where $r'_a = k_{CO}$[C]. For simplicity, the Brookhart part will be abbreviated as F_B (see eq 2).

The second part of eq 1

$$F_{cor} = \left(1 - \frac{{k_{CO}}^{-1}}{K_4 k_{C_2H_4}[C_2H_4] + {k_{CO}}^{-1}}\right)^{-1} \quad (3)$$

comes from the decarbonylation step. It indicates that nonalternation in eq 1 can be enhanced provided that F_{cor} is large enough. This can happen if the rate of decarbonylation (k_{CO}^{-1}) from D is larger than the effective propagation rate, $K_4 k_{C_2H_4}[C_2H_4]$, for ethylene insertion into the Pd−acyl bond of D. Here, K_4 is the equilibrium constant for the formation of the ethylene complex E from D and free ethene, whereas $k_{C_2H_4}$ is the rate of insertion of ethylene into the Pd−acyl bond of E. Thus, the way would be paved for obtaining nonalternating polyketones if one could lower the activation barrier for the decarbonylation of D relative to ethylene insertion into D.

Finally the percentage of nonalternation is given by

$$X_{na} = \frac{f_{na}}{1 + f_{na}} \times 100\% \quad (4)$$

We note that large values (>0.1) of f_{na} lead to a nonalternating CO/ethylene copolymerization process, whereas small values (<0.1) of f_{na} introduce alternation within the formed copolymer chain.

It should be noticed, as well, that eq 1 may be rewritten to take the following form:

$$f_{na} = \frac{r_{na}}{r_a} = \left(\frac{k'_{C_2H_4}}{k_{CO}}\frac{[C_2H_4]}{[CO]}\frac{K_1}{K_2}\right) + \left(\frac{k'_{C_2H_4}}{k_{C_2H_4}}\frac{{k_{CO}}^{-1}}{k_{CO}}\frac{K_1}{K_2 K_4[CO]}\right) = F_B + F_{cor} \quad (5)$$

thus expressing the ratio of the overall rates for the nonalternating and alternating paths, f_{na}, as a sum, instead of the product, of the Brookhart term F_B and the correction F_{cor}. However, in the present paper, we will utilize eq 1.

Results and Discussion

Thermodynamic and Kinetic Parameters for the Generic Models. We shall first turn to a discussion of CO/C_2H_4 copolymerization according to Scheme 1 as catalyzed by the generic model 2a in Figure 2, where the aryl groups on phosphorus are replaced by hydrogens. An integral part of the catalytic cycle in Scheme 1 is the uptake of a CO or ethylene monomer followed by insertion into the Pd−alkyl or Pd−acyl bond. Due to the asymmetry of the P−O chelating ligand, uptake and insertion can take place with the monomer in a position trans or cis to the chelating oxygen (Figure 3). In Table 1 are listed all of the monomer complexation energies and insertion barriers of importance for CO/C_2H_4 copolymerization. Please note that we shall talk about a Pd−alkyl or Pd−acyl bond depending on whether the last insertion involved ethylene or CO, respectively. In both cases, the actual chain attached to palladium is, of course, a polyketone.

Starting first with the ethylene uptake by the Pd−alkyl complex (A → B of Scheme 1) and subsequent insertion into the Pd−alkyl bond (B → TS-3 of Scheme 1), it is apparent

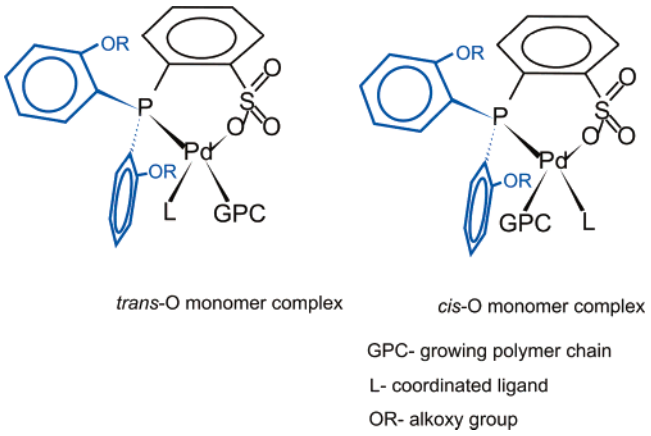

Figure 3. Schematic representation of the possible coordination modes for monomers to the studied palladium complex.

Table 1. Complexation Energies and Insertion Barriers for CO and C_2H_4 Copolymerization Catalyzed by the Generic System

	Complexation energies (kJ/mol)		Insertion barriers (kJ/mol)	
complex	cis O monomer complex[a]	trans O monomer complex[a]	cis O monomer complex[a]	trans O monomer complex[a]
C_2H_4/Pd−alkyl[b]	−29	−7.1	182.9	59.4
C_2H_4/Pd−acyl[c]	−39.2	−13.3	89.8	49.9
CO/Pd−alkyl[d]	−47.5	−48	83.9	48.3
CO/Pd−acyl[e]	−50.4	−33.8		

[a] See Figure 3. [b] For structure of Pd−alkyl/C_2H_4, see Figure 4c. [c] For structure of Pd−acyl/C_2H_4, see Figure 4k. [d] For structure of Pd−alkyl/CO, see Figure 4e. [e] For structure of Pd−acyl/CO, see Figure 4r.

from Table 1 that the adduct with ethylene coordinated cis to oxygen is preferred over the trans conformer. The optimized cis structure is shown in Figure 4c. This preference is dictated by the need for the Pd−alkyl bond to be trans to oxygen rather than to the strongly trans directing phosphorus atom,[31,32] just as in the bare Pd−alkyl complex (Figure 4a). Figure 5 displays the structure of the two conformers for the Pd−alkyl ethylene complex. It is interesting to note that ethylene in the trans conformation has moved somewhat out of the O−Pd−P coordination plane toward an axial position, whereas the equatorial site is occupied to some degree by a carbonyl oxygen from the polyketone chain. However, we shall still refer to this species as the O-trans conformer or simply π_{trans}.

It follows from Table 1 and Scheme 2 that the insertion of ethylene into the Pd−alkyl bond is more facile for the less stable π_{trans} conformer compared to that for π_{cis}. This is understandable since the Pd−alkyl bond trans to phosphorus will be activated by the strong trans-directing ability of the P atom. Assuming pre-equilibrium between π_{trans} and π_{cis} with an equilibrium constant of $K_{ct} = [\pi_{trans}]/[\pi_{cis}]$, one finds the effective rate constant of insertion, $k'_{C_2H_4}$ of Scheme 1, to be $k'_{C_2H_4} = K_{ct}k'_{tr}$, where k'_{tr} is the rate constant of insertion for the π_{trans} complex. It is readily shown[33−3633−36] that the effective barrier associated with $k'_{C_2H_4}$ of Scheme 1 can be obtained as the energy difference between π_{cis} and the insertion transition state associated with π_{trans}. In Scheme 2, the effective barrier amounts to 81.2 kJ/mol, and this is also the value given for $\Delta H^{\ddagger}_{BA}$ in Scheme 3, where we record the energetics for CO/C_2H_4 copolymerization with 2a as the catalyst.

The insertion transition state for the π_{cis} complex is shown in Figure 4o as TS-3. We note the highly activated Pd−alkyl bond trans to phosphorus. It follows from Scheme 2 that the most stable Pd−alkyl insertion product, again, has the alkyl group trans to oxygen.

Considering next CO coordination to the Pd−alkyl complex (A → C of Scheme 1), we note that the conformer π_{trans} with CO trans to oxygen is marginally more stable than the *cis* isomer π_{cis} (Table 1 and Scheme 4). Apparently, CO is a slightly more trans-directing ligand than the alkyl group. As for ethylene, and for the same reason, CO inserts (C → TS-1 → D of Scheme 1) more readily into the Pd−alkyl bond of the π_{trans} complex (Table 1 and Scheme 4). It follows from our considerations that the effective barrier of CO insertion (Scheme 4) into the Pd−alkyl bond is 48.3 kJ/mol, as recorded in Scheme 3. Also, we find CO to bind more strongly to Pd−alkyl than ethylene by 19 kJ/mol.

The optimized structure for the π_{trans} conformations is shown in Figure 4e, and the related transition state, TS-1, is in Figure 4g. The structure of the Pd−acyl complex resulting from the insertion is shown in Figure 4i. It is clearly stabilized by a chelating Pd−O bond involving a CO group on the polyketone chain. The CO insertion process (C → D of Scheme 1) is exothermic by $\Delta H_{CD} = -37.9$ kJ/mol (Scheme 4). Further, with a CO insertion activation energy of $\Delta H^{\ddagger}_{CD} = 48.3$ kJ/mol, the barrier for the reverse decarbonylation process (D → C of Scheme 1) will be $\Delta H^{\ddagger}_{DC} = 86.2$ kJ/mol (Scheme 3). It is thus clear that decarbonylation will be very slow in the CO/ethylene copolymerization catalyzed with the generic complex 2a. The reason for the high $\Delta H^{\ddagger}_{DC}$ is the strong chelating Pd−O bond shown in Figure 4i that has to be broken before the decarbonylation can take place.

After the formation of the acyl complex D, either CO or ethylene can coordinate (D → F or D → E of Scheme 1, respectively). The CO monomer prefers coordination cis to oxygen (Figure 4r). The complexation energy is $\Delta H_{DF} = -50.5$ kJ/mol (Scheme 3 and Table 1). The most stable adduct between ethylene and the Pd−acyl complex has the monomer cis to oxygen (Figure 4k) as in the corresponding complex (Figure 4c) with Pd−alkyl. The complexation energy ΔH_{DE} is −39.2 kJ/mol (Table 1 and Scheme 3).

We shall assume that the barrier of CO insertion into the Pd−acyl bond is too high for this process to proceed based on previous work by Margl et al.[16] In this case, further propagation can only take place by ethylene insertion into the Pd−acyl bond (E → TS-2 → A). As for the Pd−alkyl bond, the barrier of insertion is much lower from the π_{trans} conformer. Thus, the effective rate constant, $k_{C_2H_4}$, of Scheme 1 can be written as $k_{C_2H_4} = K'_{tc}k''_{tr}$, where k''_{tr} is the rate constant of insertion from the π_{trans} complex and K'_{tc} is the equilibrium constant $K'_{tc} = [\pi_{trans}]/[\pi_{cis}]$. The effective barrier is obtained as the energy difference between the π_{cis} conformer and the transition state for the insertion from π_{trans} as $\Delta H^{\ddagger}_{EA} = 79.1$ kJ/mol (Scheme 3). The structure TS-2 is shown in Figure 4m with the activated Pd−acyl bond trans to phosphorus.

(31) Michalak, A.; Ziegler, T. *Organometallics* **2003**, *22*, 2069−2079.
(32) Pearson, R. G. *Inorg. Chem*. **1973**, *12*, 712−713.
(33) Pollak, P. I.; Curtin, D. Y. *J. Am. Chem. Soc*. **1950**, *72*, 961−965.
(34) Curtin, D. Y.; Crew, M. C. *J. Am. Chem. Soc*. **1955**, *77*, 354−357.
(35) Seeman, J. I. *Chem Rev*. **1983**, *83*, 83−134.
(36) Adam, W.; Bach, R. D.; Dmitrenko, O.; Saha-Möller, Ch. R. *J. Org. Chem*. **2000**, *65*, 6715−6728.

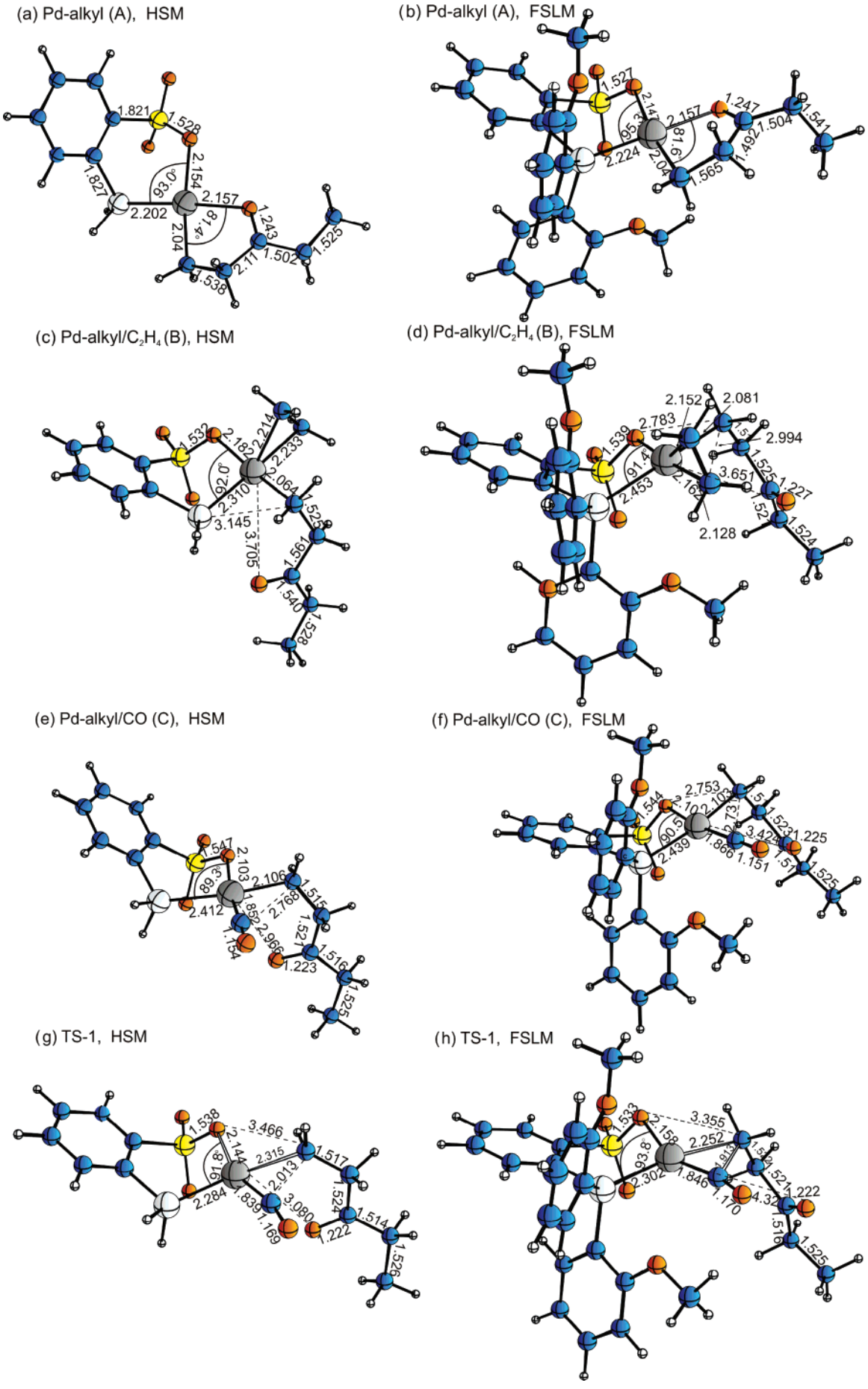
(a) Pd-alkyl (A), HSM
(b) Pd-alkyl (A), FSLM
(c) Pd-alkyl/C_2H_4 (B), HSM
(d) Pd-alkyl/C_2H_4 (B), FSLM
(e) Pd-alkyl/CO (C), HSM
(f) Pd-alkyl/CO (C), FSLM
(g) TS-1, HSM
(h) TS-1, FSLM

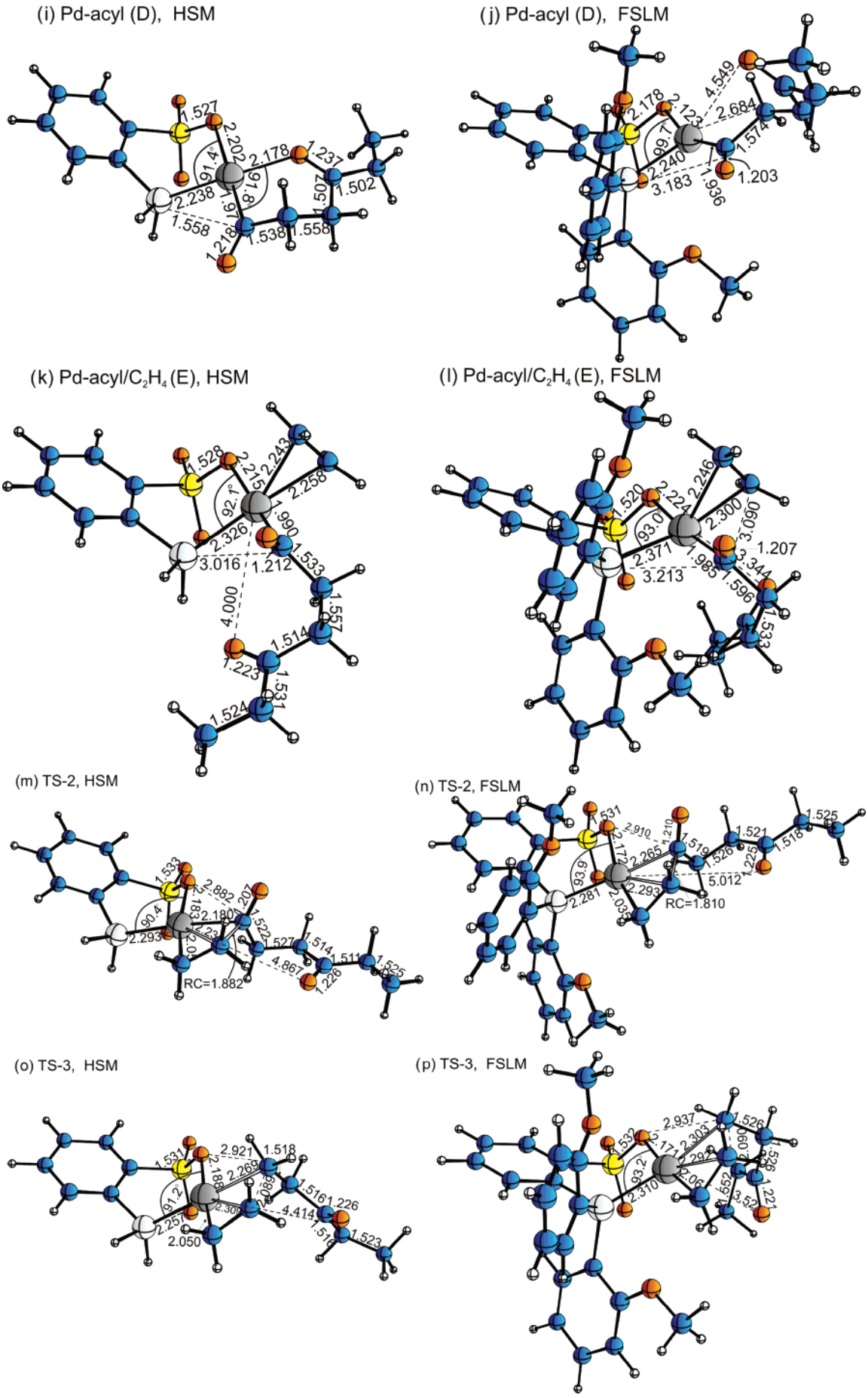
(i) Pd-acyl (D), HSM
(j) Pd-acyl (D), FSLM
(k) Pd-acyl/C_2H_4 (E), HSM
(l) Pd-acyl/C_2H_4 (E), FSLM
(m) TS-2, HSM
(n) TS-2, FSLM
(o) TS-3, HSM
(p) TS-3, FSLM
RC=1.882
RC=1.810

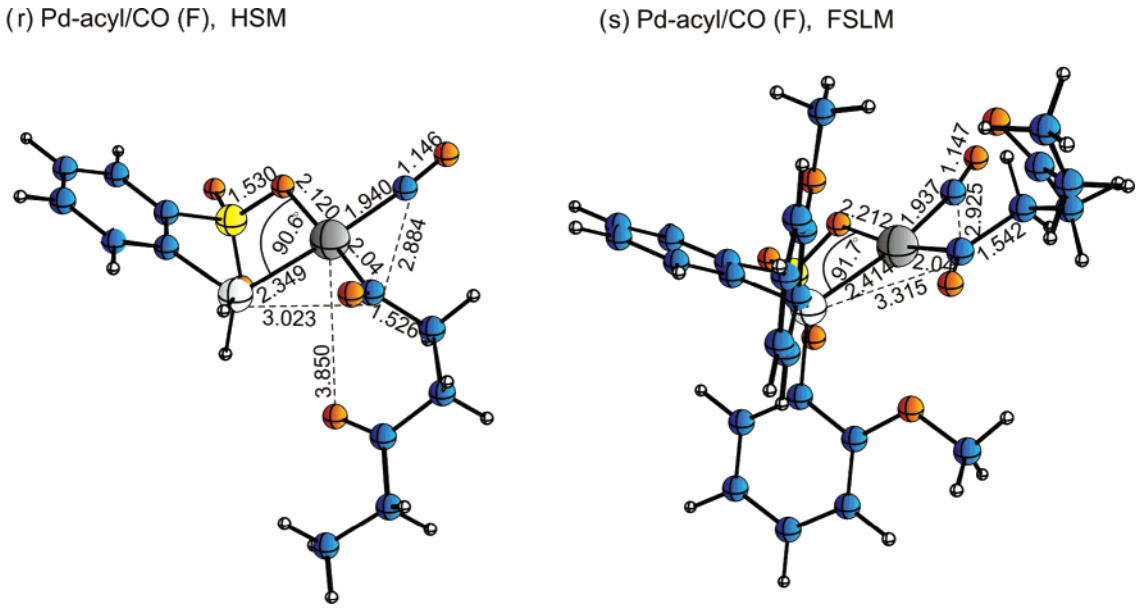

Figure 4. Optimized geometries of all stationary points corresponding to the considered catalytic cycle depicted in Scheme 1 obtained with both adopted theoretical models of the Drent's catalyst. For differentiation of atoms, see Figure 2.

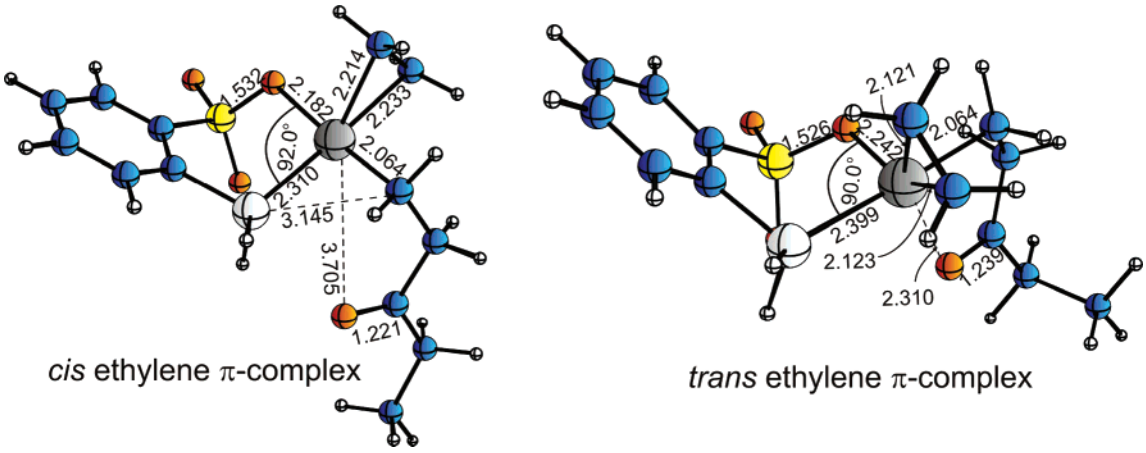

Figure 5. Side view of the optimized geometries of C_2H_4 π-complexes with Pd−alkyl modeled using the generic system. The selected structural parameters, bond lengths, and bond angles are given in angstroms and degrees, respectively. Corresponding atoms are differentiated by the color and size of the spheres. For differentiation of atoms, see Figure 2.

As it is well-known that migratory insertion reactions, being intramolecular, typically have $\Delta S^{\#} \sim 0$,[14] it is thus possible to a first approximation to neglect entropic effects and calculate the rate constants from the activation energies or, in the case of K_1/K_2, from the related heat of reaction. However, for K_4 representing ethylene dissociation from the adduct E (Scheme 1), one needs to add an entropic correction, $-T\Delta S_{ED}$, to the dissociation enthalpy, ΔH_{ED}, to evaluate K_4. On the basis of previous studies,[14,31,37] we have adopted a value of $\Delta S_{ED} = -27$ eu for all three catalysts (1a, 2a, and 2b) studied here. We find, for 2a, that $\Delta H_{ED} = 39.2$ kJ/mol (Scheme 3).

Degree of Nonalternation Predicted for HSM. Table 2 displays the calculated values for F_B, F_{cor}, and X_{na} with respect to the generic HSM system of Figure 2a.

Here, the degree of nonalternation is given according to eq 4 as $X_{na} = F_B \times F_{cor}/(1 + F_B \times F_{cor}) \times 100\%$. The factor F_B defined in eq 2 was the original measure of nonalternation given by Brookhart.[14] It is small for the generic system because $k_{CO} \gg k'_{C_2H_4}$ and $K_1/K_2 \ll 1$ (Table 2). The second factor determining X_{na} is F_{cor}. It is defined in eq 3 and takes into account decarbonylation, D → C in Scheme 1. To convert monomer pressures into concentrations, solubility of the starting monomers in methanol is taken into account by applying Henry's law constants obtained experimentally by Vavasori et al.[38] It follows from the two tables that $F_{cor} \gg 1$, which indicates that the rate of decarbonylation (k_{CO}^{-1}) of D is much larger than the rate of ethylene insertion into the Pd−acyl bond of D ($K_4 k_{C_2H_4}[C_2H_4]$).

For HSM, we find that $X_{na} \ll 1$ at 25 °C and $X_{na} \gg 1$ at higher temperature (Table 2). This would imply that the Drent's model system (HSM) is a strictly alternating CO/C_2H_4 copolymerization catalyst at low temperatures. On the other hand, the system exhibits a considerable degree of nonalternation for the temperature range of 100−120 °C, where F_B and F_{cor} are much larger than at 25 °C. The temperature increase in F_B has expected contributions from both K_1/K_2 and $k'_{C_2H_4}/k_{CO}$, whereas the increase in F_{cor} comes from the decrease in K_4 due to the

(37) Johnson, L. K.; Mecking, S.; Brookhart, M. *J. Am. Chem. Soc.* **1996**, *118*, 267−268.

(38) Vavasori, A.; Toniolo, L.; Cavinato, G. *J. Mol. Catal. A* **2004**, *215*, 63−72.

Scheme 2. Stationary Points on the Ethylene + Pd−Alkyl Potential Energy Surface for the Two Geometrical Isomers: Ethylene Coordinated Either cis or trans to Oxygen of the Bidentate Ligand[a]

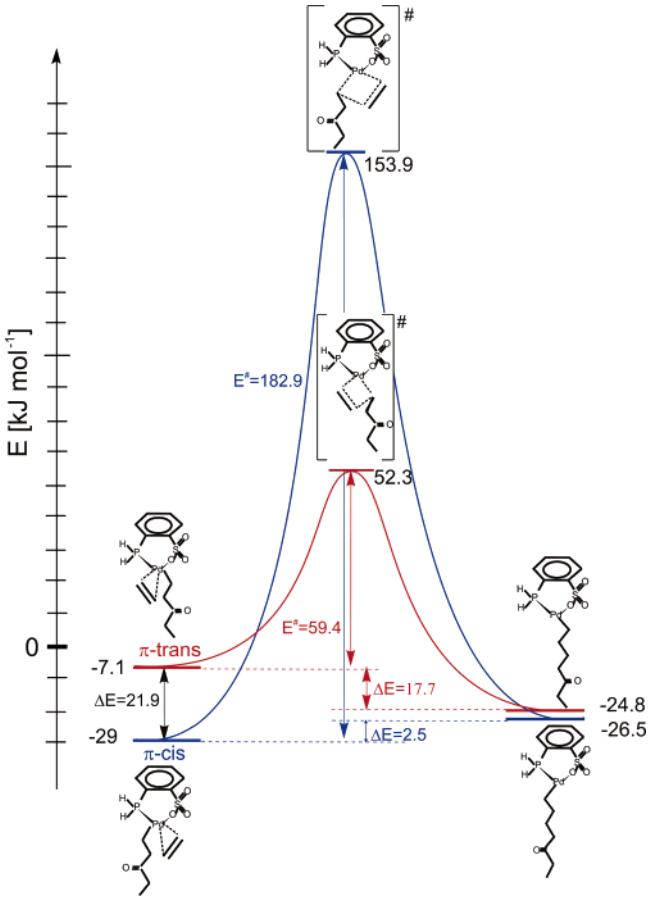

[a] The chosen reaction coordinate is the distance between the α-carbon of polymer chain and the carbon of the coordinated ethylene. The energy path for the π-trans ethylene isomer is shown in red, whereas the cis path is given in blue.

entropic factor, $-T\Delta S_{ED}$. Surprisingly, HSM exhibits at high temperatures degrees of nonalternation, X_{na}, that exceed those observed experimentally for the real (FSLM) catalyst (see Table 2).

However, an inspection of the actual rates, r_{na} and r_a, rather than their ratio would indicate that HSM has activities much smaller than those recorded experimentally for the real Drent's system (FSLM) (see Table 2). The overall rate of nonalternation (r_{na}) is seen to increase with T due to K_1/K_2, while the ratio of alternation is decreasing with T as a result of K_4 (Table 2). Overall, the activity increases slightly with temperature for HSM. We shall in the next section explore how increasing steric bulk around the metal center might influence activity and nonalternation by looking at the real Drent system (FSLM).

Degree of Nonalternation in Real System. The real Drent system (A-FSLM of Figure 4b) has two *o*-alkoxy aryl groups attached to the chelating phosphorus atom rather than two hydrogen atoms. The added bulky sidegroups make the site cis to phosphorus congested, especially after the coordination of a monomer. Thus, while the Pd−C bond is cis to phosphorus in the generic ethylene complex (B-HSM of Figure 4c), it is positioned trans in the real system (B-FSLM of Figure 4d). Further, ethylene in the cis position is forced out of the P−Pd−O coordination plane in order to reduce the steric congestion

Scheme 3. Chain Propagation Mechanism for the CO/C_2H_4 Copolymerization Reaction with the Generic System

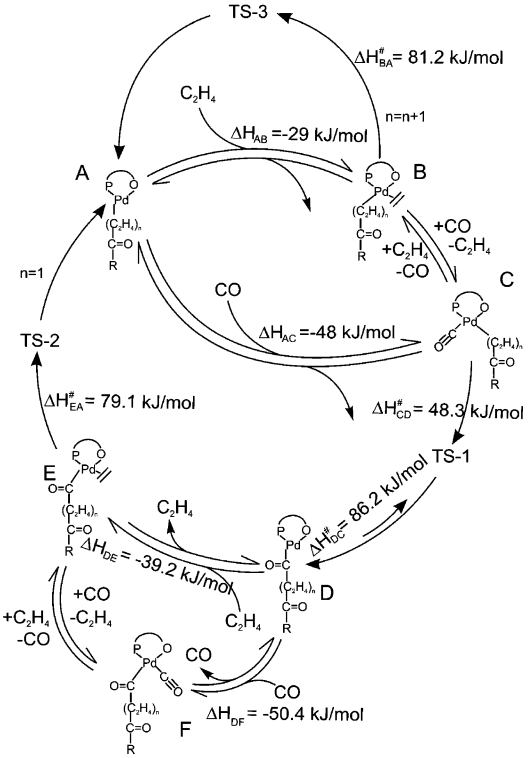

Scheme 4. Stationary Points on the Carbon Monoxide + Pd−Alkyl Potential Energy Surface for the Two Geometrical Isomers: CO Coordinated Either cis or trans to Oxygen of the Bidentate Ligand[a]

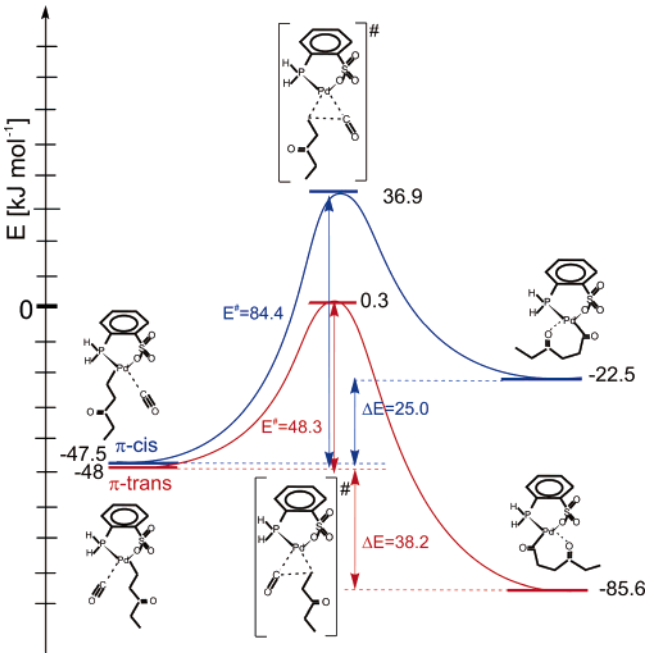

[a] The chosen reaction coordinate is the distance between the α-carbon of polymer chain and the carbon of the coordinated CO. The energy path for the CO trans isomer is shown in red, whereas the one for the CO cis is in blue.

(Figure 4d). For the corresponding CO complex, the trans coordination of the Pd−alkyl bond was already preferred electronically in the generic complex (Figure 4e), and this conformation is also adopted in the real system (Figure 4f).

Table 2. Analysis[b] of Nonalternation in CO/C_2H_4 Copolymerization Catalyzed by the Generic Drent's System[c]

T (°C)	K_1/K_2[d] ×10^4	$k'_{C_2H_4}/k_{CO}$[d] ×10^5	K_4[e] ×10^5	F_B[d] ×10^7	F_{cor}[e] ×10^{-6}	r_{na}[f]	r_a[f]	Activity[g] calcd	Activity[g] exp[h]	X^i_{na} calcd	X^i_{na} exp[h]
25	4.69	0.172	4.8	0.064	0.084	2.4×10^{-11}	4.5×10^{-8}	9×10^{-4}		0.054	
100	21.9	2.481	0.048	4.3	3.6	2.9×10^{-8}	1.9×10^{-8}	9×10^{-4}	86	60.7	4.7
110	25.7	3.272	0.035	6.6	5.3	4.7×10^{-8}	1.3×10^{-8}	1×10^{-3}	123	77.9	7.3
120	29.9	4.256	0.025	10.05	7.7	7.3×10^{-8}	9.4×10^{-9}	2×10^{-3}	108	88.5	11.0

[a] Reaction conditions according to Drent et al.:[13] 20 bar CO, 30 bar C_2H_4, 0.04 mmol (9 mg) Pd, solvent MeOH (100 mL). Solubilities of ethene and CO in methanol from Henry's law constants of the comonomers in methanol at 90 °C reported by Vavasori et al.[38] [b] For definition of different components, see eqs 1−3. [c] See 2a of Figure 2. [d] See eq 2. [e] See eq 3. [f] r_{na} and r_a are the rate of nonalternating and alternating pathways, respectively, in kg/(m^3•s). They are defined in Table 2. [g] Activity calculated as $(r_{na} + r_a) \times 3600 \times 2.2$ h × (concentration of Pd)$^{-1}$, and thus expressed as (g copolymer) × (mmol Pd × h)$^{-1}$. [h] Experimental value from ref 13. [i] See eq 4.

Scheme 5. Chain Propagation Mechanism for the CO/C_2H_4 Copolymerization Reaction with the Full-Size Ligand Model

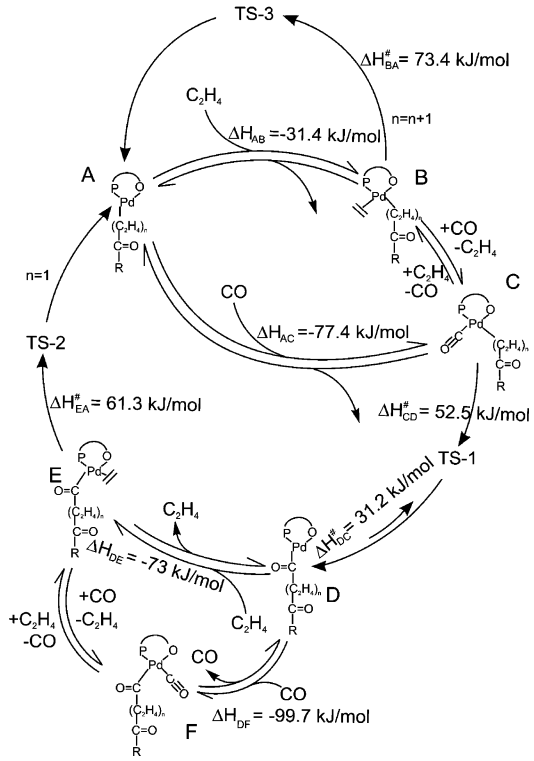

Interestingly enough, even the small CO monomer experiences some steric pressure leading to a P−Pd−CO angle larger than 90°.

Compared to the generic system, the stability of the CO complex C-FSLM is enhanced relative to the ethylene adduct (B-FSLM) by 29.4 kJ/mol (Schemes 3 and 5) due to the steric congestion which forces the larger ethylene monomer to lie out of the P−Pd−O coordination plane and the alkyl chain in the trans position.

Thus, the introduction of bulky ligands will decrease K_1/K_2 (by a factor of 10^{-4}; see Table 3) as well as the degree of nonalternation X_{na} (provided all other factors remain the same) through the Brookhart part, F_B, of eq 1 (Table 3).

In terms of relative reactivity ($k'_{C_2H_4}/k_{CO}$) of B and C, ethylene insertion has been enhanced compared to CO propagation by reducing the barrier difference $\Delta H^{\ddagger}_{BA} - \Delta H^{\ddagger}_{CD}$ from 32.9 kJ/mol in HMS to 20.9 kJ/mol in FSLM (Schemes 3 and 5). This reduction comes about as no cis/trans isomerization of the alkyl chain is required in the real system in order to reach the transition state for ethylene insertion. Thus, steric hindrance will enhance nonalternation X_{na} through the ($k'_{C_2H_4}/k_{CO}$) part of the Brookhart term F_B, provided all other factors are unchanged.

The complete Brookhart term F_B of eq 2 reflects the combined influence from the relative stability and reactivity of B and C on nonalternation, f_{na}. It follows from Table 3 that the term is reduced by introducing sterically demanding ligands through the dominating influence of the K_1/K_2 ratio. Thus considering the Brookhart term F_B alone, a full-size ligand system would lead to a reduction in nonalternation, f_{na} (Tables 2 and 3).

We shall now turn to the second term, F_{cor}, in the expression for the nonalternation fraction, f_{na}. This term is given in eq 3 and expresses the competition between the acyl complex D undergoing decarbonylation (D → C) or insertion of ethylene into the Pd−acyl bond. We note (Figure 4j) that steric congestion in D-FSLM prevents a Pd−O chelating interaction involving a carbonyl group on the polyketone chain. This is in contrast to the generic system D-HSM of Figure 4i. The result is that the real acyl complex is coordinatively unsaturated and readily can undergo decarbonylation without first having to break a Pd−O chelating bond. In fact, for D-FSLM, the decarbonylation is exothermic with $\Delta H_{DC} = -21.3$ kJ/mol and a modest barrier of $\Delta H^{\ddagger}_{DC} = 31.2$ kJ/mol (Scheme 5). This is different from D-HSM, where the process is endothermic by $\Delta H_{DC} = 35.1$ kJ/mol and the barrier is as large as $\Delta H^{\ddagger}_{DC} = 86.2$ kJ/mol. Thus, in contrast to HSM, the real system (FSLM) has the potential to exhibit a high degree of decarbonylation. Whether this will lead to nonalternation now depends on the ability of the acyl complex D to coordinate ethylene and form the complex E (K_4) as well as the rate ($k_{C_2H_4}$) by which ethylene subsequently can insert into the Pd−acyl bond.

Sterically demanding ligands attached to phosphorus have a substantial influence on the equilibrium constant K_4 between the uncoordinated Pd−acyl (D) and Pd−acyl bond to ethylene (E). Thus, the coordinatively unsaturated acyl complex (D-FSLM) will increase the affinity for ethylene coordination (D → E) to $\Delta H_{DE} = -73.0$ kJ/mol (Scheme 3), compared to $\Delta H_{DE} = -39.2$ kJ/mol in the generic system. The result is an increase in K_4 by 5 orders of magnitude (Table 3). Also, once the ethylene complex E-FSLM is formed (Figure 4l), little energy is required for the cis/trans isomerization due to the steric bulk. Thus, the barrier of insertion is decreased from $\Delta H^{\ddagger}_{EA} = 79.1$ kJ/mol in the generic system (Figure 4m) to $\Delta H^{\ddagger}_{EA} = 61.3$ kJ/mol in the real system (Figure 4n). The net result is an increase in $k_{C_2H_4}$ as well as the overall rate $K_4 k_{C_2H_4}$. In total, the ratio $k_{CO}^{-1}/(k_{CO}^{-1} + K_4 k_{C_2H_4}[C_2H_4])$ is increased by 1 order of magnitude compared to that of experiment, and that leads to a similar increase in F_{cor} and the nonalternation within the growing polyketone.

Table 3. Analysis[b] of Nonalternation in CO/C_2H_4 Copolymerization Catalyzed by the Real Drent's Catalyst[c]

T (°C)	K_1/K_2[d] ×10^7	$k'_{C_2H_4}/k_{CO}$[d] ×10^3	K_4[e]	F_B[d] ×10^9	F_{cor}[e] ×10^{-7}	r_{na}[f]	r_a[f]	Activity[g] calcd	Activity[g] exp[h]	X^i_{na} calcd	X^i_{na} exp[h]
25	0.09	0.218	6.4	0.01	0.05	5.9×10^{-8}	1.65×10^{-3}	32.65		7.5×10^{-4}	
100	3.66	1.187	0.02	3.43	1.49	7.9×10^{-7}	1.5×10^{-5}	0.32	86	4.9	4.7
110	5.39	1.415	0.01	6.02	2.12	1.1×10^{-6}	9.0×10^{-6}	0.20	123	11.3	7.3
120	7.78	1.672	0.006	10.0	3.0	1.6×10^{-6}	5.4×10^{-6}	0.14	108	23.3	11.0

[a] Reaction conditions according to Drent et al.:[13] 20 bar CO, 30 bar C_2H_4, 0.04 mmol (9 mg) Pd, solvent MeOH (100 mL). Solubilities of ethene and CO in methanol from Henry's law constants of the comonomers in methanol at 90 °C reported by Vavasori et al.[38] [b] For definition of different components, see eqs 1−3. [c] See 2a of Figure 2. [d] See eq 2. [e] See eq 3. [f] r_{na} and r_a are the rate of nonalternating and alternating pathways, respectively, in kg/(m^3•s). They are defined in Table 2. [g] Activity calculated as $(r_{na} + r_a) \times 3600 \times 2.2$ h × (concentration of Pd)$^{-1}$, and thus expressed as (g copolymer) × (mmol Pd × h)$^{-1}$. [h] Experimental value from ref 13. [i] See eq 4.

It follows from our detailed analysis that the introduction of steric hindrance has a significant influence on many of the steps in the CO/ethylene copolymerization cycle of Scheme 1. However, many of the changes introduced by the sterics have an adverse influence on X_{na}. Thus, F_B is seen to be reduced by 2 orders of magnitude, whereas F_{cor} is increased by 1 order of magnitude (Table 3). In total, X_{na} is reduced by a factor 10 compared to the generic system. However, it is gratifying that the predicted percentage of nonalternation X_{na} for the real system agrees very well with experiment over the recorded temperature range (Table 3). In addition, our kinetic model accounts well for the experimentally observed increase in nonalternation with temperature. This increase has large contributions from both K_1/K_2 and K_4. Moreover, contrary to the generic model, the overall productivity agrees satisfactorily with experimental estimates[13,39,40] (Table 3). The increase in activity of both nonalternation (r_{na}) and alternation (r_a) for the real system (FSLM) compared to those of the generic model (HSM) (Tables 2 and 3) is due to the steric bulk that prevents the chelating Pd−O interaction in the coordinatively unsaturated Pd−acyl complex D. Thus, the coordinative unsaturation facilitates ethylene coordination to D and, consequently, a higher role of alternation (r_a) through an increase in K_4. On the other hand, unsaturation also enhances the role of decarbonylation, which will lead to a higher value for r_{na}.

Concluding Remarks

We have presented a theoretical study of a Pd(II)−alkyl complex with a diphenylphosphinobenzene sulfonate coligand, FSLM of Figure 2b. This complex has recently been shown by Drent[13] et al. to copolymerize CO and ethylene in a nonalternating fashion that leads to subsequent insertions of two or more ethylene monomers. A kinetic model where all parameters (rate constants and equilibrium constants) were derived from first principle DFT calculations predicted correctly the experimentally observed percentage of nonalternation in the polyketone chain over a temperature range from 100 to 120 °C.

It follows from the proposed kinetic model that the nonalternation is a result of facile decarbonylation from the Pd−acyl complex D that is formed from insertion of CO into the Pd−alkyl bond. The decarbonylation is facilitated by the inability of the polyketone chain in D to form an extra Pd−O chelating bond, which must be broken before de-insertion of CO from the formed Pd−acyl complex. The lack of such interactions is the result of a neutral charge state of the system and the steric crowding introduced by the *o*-methoxy-substituted diphenylphosphinobenzene sulfonate coligand. However, the lack of Pd−O chelating interaction is also instrumental in facilitating the insertion of ethylene into the Pd−acyl bond of D, which will counter the influence of decarbonylation on the nonalternation to some degree (Table 3). Thus, the lack of a Pd−O chelating bond as a result of steric crowding will lead to high nonalternating (r_{na}) and alternating (r_a) activities, while maintaining a r_{na}/r_a ratio that will lead to subsequent ethylene insertions.

To summarize, both HSM and FSLM exhibit a preference for alternation at low temperature (25 °C) and a tendency for nonalternation at high temperatures (100−120 °C). However, it requires steric bulk for these systems to be sufficiently active.

Acknowledgment. Financial support from the National Sciences and Engineering Research Council of Canada (NSERC) is gratefully acknowledged. An important part of the calculations has been performed on the MACI cluster (Multimedia Advanced Computational Infrastructure) at the University of Calgary and by WestGrid computers. We would like to thank E. Drent, R. Pugh, and G. Erker for useful discussions, and Dr. Szabo for his help. T.Z. thanks to Canadian Government for a Canada Research Chair.

JA050861D

(39) Gates, D. P.; Svejda, S. A.; Oñate, E.; Killian, C. M.; Johnson, L. K.; White, P. S.; Brookhart, M. *Macromolecules* **2000**, *33*, 2320−2334.
(40) Harley, A. K.; Nowack, R. J.; Reiger, B. *Organometallics* **2005**, *24*, 2755−2763.